Draft version October 20, 2018
Typeset using LaTeX **twocolumn** style in AASTeX62

A Theory on Stellar Interactions with Protoplanetary Disks

Isaiah I. Tristan[1] and Andrea Isella[1]

[1] *Rice University*
6100 Main Street
Houston, TX 77005-1892, USA

ABSTRACT

[ADD ONCE FINISHED]

Keywords: astrometry — catalogs — protoplanetary disks

1. INTRODUCTION

In recent years, observations through the Atacama Large Millimeter/submillimeter Array (ALMA) and the Submillimeter Array (SMA) have discovered protoplanetary disks with asymmetries in their dust. These often come in the form of uneven spirals or crescents where material is focused on one side (Isella & Turner 2016). As this is a relatively newly observed phenomena, the origin of these asymmetries has not been settled. A few theories include protoplanets trapping and dragging dust as they orbit, gaps caused by photoevaporation, viscosity gradients, gravitational instabilities, or protoplanet collisions (van der Marel et al. 2013). While protoplanets gravitationally shepherding dust is currently the most studied theory, the timescales for the asymmetries in these models are inconsistent with those of planet formation Citation? Maybe the 2013 van der Marel?.

Our theory is that these asymmetries are instigated by gravitational interactions with neighboring stars. Should a star pass close enough to the protoplanetary disk, its gravitational pull will cause perturbations, which will lead to dust and gas buildup in a certain area. Furthermore, we have seen binary-driven artifacts in protoplanetary disks (Wagner et al. 2018), showing that close-range interactions with other stars in general do affect structures of disks.

Finish this to "2. METHODS" later, add section about current simulations Given the standard thought of star distribution, we expect few interactions in the past years. Assuming that the asymmetrical disks would be able to smoothen out over time, we expect to see this gravitational interaction within the past few hundred thousand years or so. However, should the interaction itself induces pressure gradient and promote dust trapping in the disk, the asymmetries could survive much longer. If interactions seem likely but timescales seem off, we must consider a combined contribution from gravitational interactions and other theories, but for this project, we will only consider our current theory.

Corresponding author: Andrea Isella
isella@rice.edu

2. METHODS

Our objective is to determine if a star with a protoplanetary disk could have interacted with a neighboring star in the past one million years and if stars with asymmetrical disks have more potential interactions using the data available in the *Gaia* Data Release 2 (DR2) Catalog.

2.1. *Selecting a Sample of Stars with Protoplanetary Disks*

Remove HT Lup and AS 205 on account of being binaries. Consider separate section? Treat HD 163296 separately on account of dense field

We collected a sample of 37 stars bearing protoplanetary disks to test our theory. Of these, ?? showed azimuthal asymmetries in the form of crescent, blobby, or spiral structures, while the others were azimuthally symmetric. We then obtained their positions (α and δ, in degrees), proper motions ($\mu_\alpha \cos(\delta)$ and μ_δ, in mas yr $^{-}1$), and parallaxes (ϖ in mas) along with their associated errors from the *Gaia* DR2 Catalog (Lindegren et al. 2018), shown in Table 1.

2.2. *Querying Regions Around Sample Stars*

Table 1. Properties of Known Stars with Protoplanetary Disks

Name	α (J2000)	δ (J2000)	ϖ (mas)	d (pc)	$\mu_\alpha \cos(\delta)$ (mas yr^{-1})	μ_δ (mas yr^{-1})	V_{helio} (km s^{-1})	V_r Ref.
Asymmetrical Disks								
LkHα 330	03 45 48.280	+32 24 11.851	3.22 ± 0.08	$310.95^{+7.80}_{-7.43}$	4.58 ± 0.12	-5.66 ± 0.09	14.68 ± 1.11	1
AB Aur	04 55 45.845	+30 33 04.293	6.14 ± 0.06	$162.87^{+1.53}_{-1.50}$	3.93 ± 0.10	-24.11 ± 0.07	8.90 ± 0.90	2
MWC 758	05 30 27.528	+25 19 57.082	6.24 ± 0.07	$160.24^{+1.74}_{-1.71}$	3.59 ± 0.11	-26.75 ± 0.08	...	
HD 100546	11 33 25.440	-70 11 41.239	9.09 ± 0.05	$110.02^{+0.62}_{-0.61}$	-38.59 ± 0.08	-0.24 ± 0.08	15.74 ± 2.00	3, §, †
PDS 70	14 08 10.154	-41 23 52.576	8.82 ± 0.04	$113.43^{+0.52}_{-0.52}$	-29.66 ± 0.07	-23.82 ± 0.06	3.13 ± 1.40	1
SAO 206462	15 15 48.445	-37 09 16.026	7.37 ± 0.08	$135.77^{+1.44}_{-1.41}$	-19.11 ± 0.11	-23.14 ± 0.08	2.96 ± 1.00	4, §, †
HD 142527	15 56 41.888	-42 19 23.245	6.36 ± 0.05	$157.33^{+1.18}_{-1.16}$	-11.30 ± 0.09	-26.34 ± 0.06	-0.23 ± 1.18	1
HD 143006	15 58 36.912	-22 57 15.221	6.02 ± 0.15	$166.09^{+4.13}_{-3.94}$	-10.88 ± 0.11	-20.96 ± 0.06	-3.26 ± 0.68	1
EM* SR 21A	16 27 10.277	-24 19 12.620	7.23 ± 0.06	$138.40^{+1.09}_{-1.08}$	-5.61 ± 0.14	-29.08 ± 0.09	-7.34 ± 2.00	4, §, †
IRAS 16245-2423	16 27 37.191	-24 30 35.031	7.44 ± 0.12	$134.45^{+2.12}_{-2.06}$	-9.19 ± 0.23	-23.99 ± 0.18	-5.75 ± 1.00	4, §, †
Symmetrical Disks								
LkCa 15	04 39 17.791	+22 21 03.387	6.29 ± 0.05	$158.87^{+1.22}_{-1.21}$	10.47 ± 0.13	-17.38 ± 0.06	17.65 ± 0.03	5
CQ Tau	05 35 58.467	+24 44 54.086	6.13 ± 0.08	$163.12^{+2.21}_{-2.16}$	2.56 ± 0.13	-26.03 ± 0.11	31.40 ± 5.35	1
TW Hya	11 01 51.905	-34 42 17.031	16.64 ± 0.04	$60.09^{+0.15}_{-0.15}$	-68.39 ± 0.05	-14.02 ± 0.06	12.34 ± 0.03	1
HD 97048	11 08 03.310	-77 39 17.491	5.41 ± 0.04	$184.83^{+1.33}_{-1.32}$	-22.44 ± 0.06	1.30 ± 0.06	18.00 ± 3.00	6
RX J1604.3-2130A	16 04 21.654	-21 30 28.549	6.66 ± 0.06	$150.12^{+1.28}_{-1.26}$	-12.33 ± 0.10	-23.83 ± 0.05	-7.60 ± 1.63	1
RX J1615.3-3255	16 15 20.233	-32 55 05.097	6.34 ± 0.04	$157.69^{+0.90}_{-0.89}$	-8.05 ± 0.08	-23.45 ± 0.07	-2.40 ± 1.00	7
DoAr 25	16 26 23.691	-24 43 13.886	7.22 ± 0.08	$138.46^{+1.48}_{-1.45}$	-7.83 ± 0.17	-26.29 ± 0.13	-12.64 ± 5.75	1
AS 209	16 49 15.303	-14 22 08.642	8.27 ± 0.06	$120.98^{+0.91}_{-0.90}$	-7.42 ± 0.12	-23.73 ± 0.07	-8.96 ± 0.40	8, §
HD 163296	17 56 21.288	-21 57 21.872	9.85 ± 0.11	$101.50^{+1.19}_{-1.16}$	-7.61 ± 0.15	-39.42 ± 0.12	-6.32 ± 8.00	8, §, ‡
HD 169142	18 24 29.779	-29 46 49.328	8.77 ± 0.06	$113.96^{+0.83}_{-0.82}$	-2.32 ± 0.11	-37.80 ± 0.09	-3.00 ± 2.00	6
NEED TO CHECK								
HT Lup	15 45 12.867	-34 17 30.646	6.49 ± 0.06	$154.19^{+1.45}_{-1.42}$	-13.62 ± 0.13	-21.60 ± 0.08	-4.30 ± 1.80	9
GW Lup	15 46 44.729	-34 30 35.677	6.41 ± 0.06	$155.89^{+1.35}_{-1.33}$	-14.03 ± 0.10	-23.36 ± 0.07	-3.30 ± 1.90	9
IM Lup	15 56 09.206	-37 56 06.126	6.31 ± 0.05	$158.45^{+1.36}_{-1.33}$	-12.09 ± 0.12	-23.72 ± 0.07	-0.50 ± 1.30	9
HD 142666	15 56 40.022	-22 01 40.004	6.74 ± 0.05	$148.28^{+1.17}_{-1.15}$	-13.05 ± 0.11	-22.16 ± 0.06	-7.00 ± 2.70	10
RU Lup	15 56 42.310	-37 49 15.473	6.27 ± 0.07	$159.57^{+1.73}_{-1.70}$	-11.55 ± 0.14	-23.23 ± 0.09	3.30 ± 1.80	9
Sz 129	15 59 16.471	-41 57 10.300	6.18 ± 0.05	$161.68^{+1.33}_{-1.31}$	-10.46 ± 0.09	-23.11 ± 0.06	3.20 ± 2.50	9
MY Lup	16 00 44.519	-41 55 30.931	6.39 ± 0.05	$156.58^{+1.17}_{-1.16}$	-11.43 ± 0.10	-23.40 ± 0.07	4.40 ± 2.10	9
Sz 114	16 09 01.848	-39 05 12.416	6.16 ± 0.05	$162.25^{+1.41}_{-1.39}$	-9.66 ± 0.09	-23.93 ± 0.06	4.00 ± 2.40	9
AS 205	16 11 31.360	-18 38 25.775	7.82 ± 0.10	$127.93^{+1.62}_{-1.58}$	-7.45 ± 0.20	-26.89 ± 0.14	-7.06 ± 0.18	11, §
EM* SR 4	16 25 56.165	-24 20 48.239	7.43 ± 0.05	$134.60^{+0.83}_{-0.82}$	-7.48 ± 0.13	-26.61 ± 0.08	-6.29 ± 1.50	8, §, ‡
Elias 2-20	16 26 18.878	-24 28 19.698	7.22 ± 0.23	$138.42^{+4.50}_{-4.22}$	-8.99 ± 0.64	-27.34 ± 0.37	-6.27 ± 1.00	8, §, ‡
Elias 2-24	16 26 24.089	-24 16 13.456	7.34 ± 0.11	$136.22^{+2.05}_{-1.99}$	-8.83 ± 0.25	-24.20 ± 0.16	-7.33 ± 2.00	8, §, ‡
Elias 2-27	16 26 45.032	-24 23 07.808	8.63 ± 0.98	$115.88^{+14.77}_{-11.77}$	-8.21 ± 2.89	-27.29 ± 1.73	-5.81 ± 2.00	8, §, ‡
DoAr 33	16 27 39.012	-23 58 18.708	7.15 ± 0.05	$139.92^{+1.08}_{-1.06}$	-6.98 ± 0.12	-27.08 ± 0.07	...	
WSB 52	16 27 39.429	-24 39 15.527	7.30 ± 0.09	$137.02^{+1.76}_{-1.71}$	-6.31 ± 0.21	-25.33 ± 0.13	-6.26 ± 2.50	8, §, ‡
DoAr 44	16 31 33.463	-24 27 37.158	6.85 ± 0.05	$145.91^{+1.00}_{-0.98}$	-6.10 ± 0.13	-24.21 ± 0.10	-6.07 ± 3.00	4, §, †
Wa Oph 6	16 48 45.632	-14 16 35.849	8.07 ± 0.05	$123.86^{+0.72}_{-0.71}$	-8.41 ± 0.10	-23.12 ± 0.05	-8.97 ± 0.50	8, §, ‡

NOTE—‡ indicates that V_r and its error were estimated from a provided spectra graph † indicates that only the error was estimated. § indicates that the reported value was in the LSR frame.

References— (1) Gaia Collaboration et al. (2018), (2) Anderson & Francis (2012), (3) Wright et al. (2015), (4) van der Marel et al. (2016), (5) Nguyen et al. (2012), (6) Carmona et al. (2011), (7) Wichmann et al. (1999), (8) Reboussin et al. (2015), (9) Frasca et al. (2017), (10) Alecian et al. (2013), (11) Salyk et al. (2014)

For each star in the sample, we checked how the star would move across the 2D plane of the sky in the past one million years, using Equations 1 and 2, and converting the units of proper motions to degrees per year. Then, we took the midpoint of this motion and queried a circle with a radius much larger than the total travel distance. This is to ensure than we are able to find as many potential interactions as possible for the stars traveling in any direction.

$$\alpha_t = \alpha_0 - \mu_\alpha \cos(\delta) t \quad (1)$$

$$\delta_t = \delta_0 - \mu_\delta t \quad (2)$$

Since we are exploring this theory, we eliminate stars with parallax errors larger than 10% of their parallax. While this may bias our data towards brighter and well-behaved stars, this gives us more probable data, which

is not necessarily unwanted. We also cut stars with parallaxes < 2.0, as their corresponding distances will be much further than any of our sample.

2.3. *Distance Determination*

We can determine distances to our objects based on the parallaxes obtained from the Gaia DR2 catalog, but there are a few different methods. The first, is to use Equation 3, which will give us the distance to stars with little to no errors.

$$d = \frac{1}{\varpi} \tag{3}$$

The next is to use a Bayesian approach to determining distances, as recommended by Luri et al. (2018). However using the Exponentially Decreasing Space Density Prior with the tools provided for quick calculations, the outputs are mainly consistent with Equation 3. It is noted using Equation 3 for stars with whose parallax error is within 20% and distance is within 1 kpc should give a reasonable distance estimations. As a proof of concept, we test the Bayesian approach for distances of our search sample and find that it returns similar distances and errors on average (within 0.1% and 3.9% respectively, using provided tools).

2.4. *Astrometric Error Considerations*

For stars whose motions did not fit Gaia's astrometric solution, values were inflated to remedy the situations, and this was reported as the excess astrometric noise (ε_i in mas). While this value is 0 for well-behaved stars, it is large for binary stars with moderate acceleration, so to account for this, we add the astrometric error in quadrature to the proper motions and parallaxes using Equation 4. We do this after cuts so that this only adds to the potential interactions, instead of cutting out good data also.

$$\sigma_{new} = \sqrt{\sigma^2 + \varepsilon_i^2} \tag{4}$$

2.5. *Potential Interactions in 2D*

We first selected stars whose parallaxes overlap ($\pm$ errors and a 15 pc past-motion buffer) with the sample star's so that we are only working with stars in the sample star's neighborhood.

We then used proper motions and errors to create areas of possible positions for each star and the target. If any star's area lied within a defined interaction radius of 1,000 AU of their target's, we considered them for further vetting.

Even if the areas of possible positions overlapped, it was possible that the objects were not in the same area at the same time. So, using a relatively small time interval of 50 years, we broke the areas into lines of possible positions corresponding to each time. Any star whose lines of positions still fell within the interaction radius were considered 2D candidates for interaction.

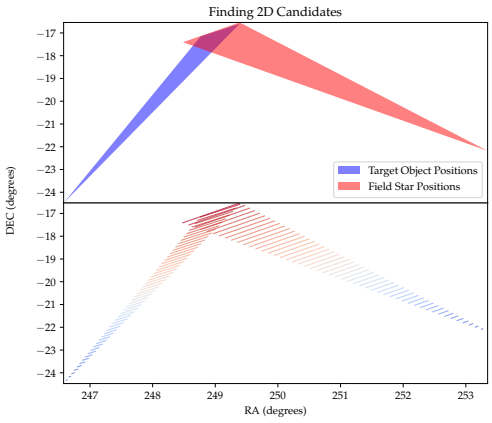

Figure 1. If the possible positions of the stars overlapped or were within the interaction radius , the stars were then time stepped to ensure the positions overlapped at the same time.
Bottom: the color shadings represent different time steps.

It should be noted that the 2D-projection of the sky is not entirely accurate, and the further they travel, the more the error propagates. However, most of our test subjects are at a far enough distance that they do not move significantly across the sky and the approximation is reasonable for this vetting, as most of the queried stars did not have radial velocities (RV) available. In addition to this, proper motions are not completely intrinsic to their stars (as there is a small contribution from the motion of our own solar system), but for our timescales, we consider the error caused by this to be negligible. Special care was taken for stars that crossed boundary the 0°/360° RA boundaries, but none of our queries reached the 90°/-90° DEC boundaries significantly.

2.6. *Radial Velocities Collection and Corrections*

After obtaining the list of 2D candidates, we searched the literature for RV data for any stars that did not have it available through the Gaia DR2 catalog. When needed, we converted V_{LSR} data to V_{helio} (largely consistent with DR2's solar barycentric frame) using Equation 5 (derived from Mihalas & Binney (1981)). Note, $V_\odot = 20$ km s^{-1}, $\alpha_0 = 270°$, $\delta_0 = +30°$, and B1950 coordinates are used.

$$V_{helio} = V_{LSR} - V_\odot[\cos(\alpha - \alpha_0)\cos\delta\cos\delta_0 + \sin\delta\sin\delta_0] \tag{5}$$

After this, we had obtained RVs for a total of 378 stars, with ?? being from other sources (listed in Table 2).

2.7. *3D Separation for Potential Interactions*

For the 2D candidates that had RV data available, we performed a much more rigorous test in 3D-space. With proper motions, parallaxes, and radial velocities, we created a complete picture of how the stars have moved in the past. The first step was to convert positions and velocities to Cartesian equatorial coordinates, using Equations 6, 7, and 8.

$$x_0 = d\cos\alpha\cos\delta \tag{6}$$
$$y_0 = d\sin\alpha\cos\delta \tag{7}$$
$$z_0 = d\sin\delta \tag{8}$$

We then obtained transverse velocities in RA and DEC by using Equations 9 and 10 and converted them kilometers per second (km $\sec^{-1}$) by multiplying them by a constant factor of $A = 4.744 * 10^{-3}$.

$$V_{T\alpha} = A\mu_\alpha d \tag{9}$$
$$V_{T\delta} = A\mu_\delta d \tag{10}$$

We then used the transverse and radial velocities to determine the Cartesian velocities using Equations 11, 12, and 13.

$$v_x = V_r\cos\delta\cos\alpha - V_{T\alpha}\sin\alpha - V_{T\delta}\sin\delta\cos\alpha \tag{11}$$
$$v_y = V_r\cos\delta\sin\alpha + V_{T\alpha}\cos(\alpha) - V_{T\delta}\sin\delta\sin\alpha \tag{12}$$
$$v_z = V_r\sin\delta + V_{T\delta}\cos\delta \tag{13}$$

Since these positions are in parsecs, we converted the Cartesian equatorial velocities from km $\sec^{-1}$ to pc yr^{-1} by multiplying a factor of $B = 1.022 * 10^{-6}$ to match. Finally, we time-stepped the system using Equations 14, 15, and 16, which are similar to the 2D ones.

$$x_t = x_0 - Bv_x t \tag{14}$$
$$y_t = y_0 - Bv_y t \tag{15}$$
$$z_t = z_0 - Bv_z t \tag{16}$$

Given our spatial understanding of stars, we expected there to be few gravitational interactions between them in 3D space, and extrapolated this motion linearly for our time frame without worrying about gravitational interactions from others stars changing their path.

For each candidate with all data available, we created a range of possible distances given its error and broke it into points. For each point, we calculated Cartesian velocity ranges and positions, defined a line of motion in 3D space based on the line of motion, defined a radius of uncertainty given maximum errors, and essentially created a volume of possible positions for each time interval. Finally, these volumes were compared, and if a star's lied within the interaction radius to the target's, the object was considered a true candidate for interaction.

2.8. *Separation Uncertainty*

Need to add paragraph going through the process. Potentially graph showing how the uncertainty is affected/distributed?

$$f = ax \pm by \qquad \sigma_f^2 = a^2\sigma_x^2 + b^2\sigma_y^2 \tag{17}$$
$$f = xy \qquad \frac{\sigma_f^2}{f^2} = \frac{\sigma_x^2}{x^2} + \frac{\sigma_y^2}{y^2} \tag{18}$$
$$f = x^c \qquad \frac{\sigma_f}{f} = c\frac{\sigma_x}{x} \tag{19}$$

$$\sigma_{x_0} = \sigma_d|\cos\alpha\cos\delta| \tag{20}$$
$$\sigma_{y_0} = \sigma_d|\sin\alpha\cos\delta| \tag{21}$$
$$\sigma_{z_0} = \sigma_d|\sin\delta| \tag{22}$$

$$\sigma_{V_{T\alpha}} = |AV_{T\alpha}|\sqrt{\left(\frac{\sigma_{\mu_\alpha}}{\mu_\alpha}\right)^2 + \left(\frac{\sigma_d}{d}\right)^2} \tag{23}$$
$$\sigma_{V_{T\delta}} = |AV_{T\delta}|\sqrt{\left(\frac{\sigma_{\mu_\delta}}{\mu_\delta}\right)^2 + \left(\frac{\sigma_d}{d}\right)^2} \tag{24}$$

$$a = \cos\delta\cos\alpha \qquad b = \sin\delta\cos\alpha$$
$$c = \cos\delta\sin\alpha \qquad f = \sin\delta\sin\alpha$$

$$\sigma_{v_x} = \sqrt{(\sigma_{V_r}a)^2 + (\sigma_{V_{T\alpha}}\sin\alpha)^2 + (\sigma_{V_{T\delta}}b)^2} \tag{25}$$
$$\sigma_{v_y} = \sqrt{(\sigma_{V_r}c)^2 + (\sigma_{V_{T\alpha}}\cos\alpha)^2 + (\sigma_{V_{T\delta}}f)^2} \tag{26}$$
$$\sigma_{v_z} = \sqrt{(\sigma_{V_r}\sin\delta)^2 + (\sigma_{V_{T\delta}}\cos\delta)^2} \tag{27}$$

$$\sigma_{x_t} = \sqrt{\sigma_{x_0}^2 + (Bt\sigma_{v_x})^2} \tag{28}$$
$$\sigma_{y_t} = \sqrt{\sigma_{y_0}^2 + (Bt\sigma_{v_y})^2} \tag{29}$$
$$\sigma_{z_t} = \sqrt{\sigma_{z_0}^2 + (Bt\sigma_{v_z})^2} \tag{30}$$

$$S = \sqrt{(x_1 - x_2)^2 + (y_1 - y_2)^2 + (z_1 - z_2)^2} \tag{31}$$

$$\sigma_S = S^{-1}((x_1 - x_2)^2(\sigma_{x_1}^2 + \sigma_{x_2}^2) + (y_1 - y_2)^2(\sigma_{y_1}^2 + \sigma_{y_2}^2) + (z_1 - z_2)^2(\sigma_{z_1}^2 + \sigma_{z_2}^2))^{\frac{1}{2}} \tag{32}$$

Table 2. Radial Velocities from Other Sources

Gaia DR2	Other Name	V_{helio} (km s^{-1})	V_r Ref.
a	a	a	a

NOTE—§ indicates that the reported value was in the LSR frame.

References— (1) , (2) , (3) , (4) , (5) , (6) , (7) , (8) , (9) , (10) , (11)

2.9. *Comparing Model and Statistical Separation*

For these purposes, it is necessary to combine using a 3d model and statistical uncertainty to determine potential interactions. The cartesian coordinates inherit uncertainties from their distances, which can lead to a smaller present-time separation than uncertainty. As we can see the objects are not within 1,000 AU of each other, we use the physical model to determine at which times interactions would be possible. If the physical and statistical models match timeframes, the interactions are to have occurred within 1σ. Interactions that did not meet this were all found to be within 2σ.

3. RESULTS

We performed our interaction test on a **sample of 37 stars** with protoplanetary disks, whose kinematic properties are shown in Table 1. We theorize that for a neighboring star to have a significant impact on a protoplanetary disk, it would have to pass within an **interaction radius of 1,000 AU**. We also choose the assumption that asymmetries would keep intact for a **timeframe of one million years**, and for testing we break this time into **intervals of 50 years**.

3.1. *Interaction Candidates*

Talk about number of candidates, percentages of how many stars bearing disks had potential interactions, and how many per symm/asymm

4. DISCUSSION & CONCLUSIONS

1. Do we think this theory is reasonable? Why/why not?
2. Are there more potential interactions with asym or sym disks? are there enough possibilities without RV data to take into consideration?
3. What do we expect to build upon this?

This work has made use of data from the European Space Agency (ESA) mission Gaia (https://www.cosmos.esa.int/gaia), processed by the Gaia Data Processing and Analysis Consortium (DPAC, https://www.cosmos.esa.int/web/gaia/dpac/consortium). Funding for the DPAC has been provided by national institutions, in particular the institutions participating in the Gaia Multilateral Agreement.

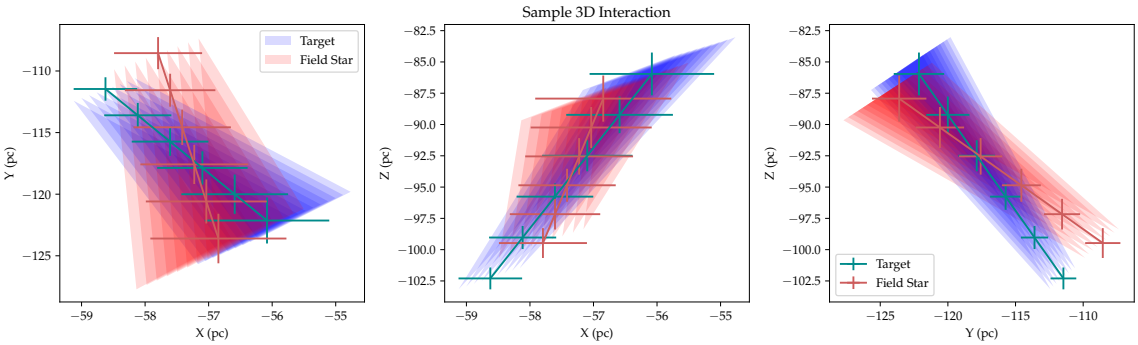

Figure 2. The shaded areas represent the potential volume covered by the 3D-Cartesian space model in the solar barycentric frame, while the solid lines represent the uncertainties of each coordinate. When both volumes and uncertanties overlapped in the same timeframe, stars were considered true candidates for interaction.

APPENDIX

A. ABBREVIATIONS & MATHEMATICAL SYMBOLS

Table A.1. List of short forms used.

Abbreviation	Long Form
ε_i	Astrometric Excess Noise
D	Astrometric Excess Noise Significance
AU	Astronomical Unit
x, y, z	Cartesian Positions
$v_{x,y,z}$	Cartesian Velocities
DEC, δ	Declination
d	Distance
$T_{\rm eff}$	Effective Temperature
K	Kelvin
km sec^{-1}	Kilometers per Second
log(g)	Log Surface Gravity
$M_\odot$	Mass of the Sun
[Fe/H]	Metallicity
mas yr^{-1}	Milliarcseconds per Year
ϖ	Parallax
pc	Parsecs
$\mu_\alpha \cos(\delta)$, μ_δ	Proper Motion
RA, α	Right Ascension
RV, V_r	Radial Velocity
V_{helio}	Heliocentric Radial Velocity
$R_\odot$	Radius of the Sun
t	Time
V_T	Transverse Velocity
$V_\odot$	Velocity of the Sun

Table 3. Possible Interactions (1σ, No Astrometric Error)

Gaia DR2	Other Name	t_{range} (kyr)	$t_{S_{min}}$ (kyr)	S_{min} (pc)	$\sigma_{S_{min}}$ (pc)
HD 142527					
5995094095435598848	Sz 133	0-753	262	4.59	7.66
CQ Tau					
3423110173528595584		321-370	362	1.00	1.89
HD 97048					
5201153791426217472	2MASS J11072040-7729403	409-1000	1000	0.69	1.92
RX J1604.3-2130A					
6242866601193873536	HD 145188	409-545	446	1.59	1.71
RX J1615.3-3255					
6036464972760199040		114-617	321	3.61	6.61
DoAr 25					
6049117843329171968	2MASS J16264429-2443141	6-929	257	0.07	1.18
6049137943776073216	ISO-Oph 30	0-89	0	1.99	2.40
HT Lup					
6014696875913435520	2MASS J15450887-3417333	0-958	184	0.27	3.12
GW Lup					
6014696875913435520	2MASS J15450887-3417333	0-1000	0	1.42	2.92
Sz 119					
5995094095435598848	SZ 133	311-437	318	7.98	7.99
Sz 114					
5997484502428382592		212-382	297	3.47	5.45
5997889947346499840		640-738	689	1.01	1.53
Elias 2-20					
6046401598639787264		321-461	410	1.83	3.29
6049137943776073216	ISO-Oph 30	0-1000	70	1.83	4.02
6050945747052676352	* rho Oph C	397-1000	854	1.18	3.87
Elias 2-24					
6049137943776073216	ISO-Oph 30	0-1000	418	0.10	2.31
Elias 2-27					
1199629656205894656	* r Her	956-1000	1000	5.50	8.73
4113859073572108032		339-668	446	3.29	8.44
4122145719085789824		551-771	655	2.02	8.24
4323764300104442240		507-1000	1000	2.30	9.62
4325143328203609600		599-667	665	8.59	8.62
6046310274762375808		573-1000	972	6.44	9.35
6050072661804674048		140-327	275	6.40	8.22
6050875614529786752	VSS II-28	311-1000	1000	7.71	10.27
6247463075195845504		545-1000	906	2.01	8.29
6249150756825746304		574-1000	736	5.89	8.69
WSB 52					
6049137943776073216	ISO-Oph 30	0-1000	415	0.66	1.85

REFERENCES

Alecian, E., Wade, G. A., Catala, C., et al. 2013, MNRAS, 429, 1001

Anderson, E., & Francis, C. 2012, Astronomy Letters, 38, 331

Carmona, A., van der Plas, G., van den Ancker, M. E., et al. 2011, A&A, 533, A39

Dahm, S. E., Slesnick, C. L., & White, R. J. 2012, ApJ, 745, 56

de Bruijne, J. H. J., & Eilers, A.-C. 2012, A&A, 546, A61

Frasca, A., Biazzo, K., Alcalá, J. M., et al. 2017, A&A, 602, A33

Gaia Collaboration, Clementini, G., Eyer, L., et al. 2017, A&A, 605, A79

Gaia Collaboration, Brown, A. G. A., Vallenari, A., et al. 2018, arXiv:1804.09365

Isella, A., & Turner, N. 2016, arXiv:1608.05123

Katz, D., Sartoretti, P., Cropper, M., et al. 2018, arXiv:1804.09372

Lindegren, L., Hernandez, J., Bombrun, A., et al. 2018, arXiv:1804.09366

Luri, X., Brown, A. G. A., Sarro, L. M., et al. 2018, arXiv:1804.09376

Mihalas, D., & Binney, J. 1981, San Francisco, CA, W. H. Freeman and Co., 1981. 608 p.,

Nguyen, D. C., Brandeker, A., van Kerkwijk, M. H., & Jayawardhana, R. 2012, ApJ, 745, 119

Reboussin, L., Guilloteau, S., Simon, M., et al. 2015, A&A, 578, A31

Salgado, J., González-Núñez, J., Gutiérrez-Sánchez, R., et al. 2017, Astronomy and Computing, 21, 22

Salyk, C., Pontoppidan, K., Corder, S., et al. 2014, ApJ, 792, 68

Soubiran, C., Jasniewicz, G., Chemin, L., et al. 2018, arXiv:1804.09370

van der Marel, N., van Dishoeck, E. F., Bruderer, S., et al. 2013, Science, 340, 1199

van der Marel, N., van Dishoeck, E. F., et al. 2016, A&A, 585, A58

Wagner, K., Dong, R., Sheehan, P., et al. 2018, ApJ, 854, 130

Wichmann, R., Covino, E., Alcalá, J. M., et al. 1999, MNRAS, 307, 909

Wright, C. M., Maddison, S. T., Wilner, D. J., et al. 2015, MNRAS, 453, 414